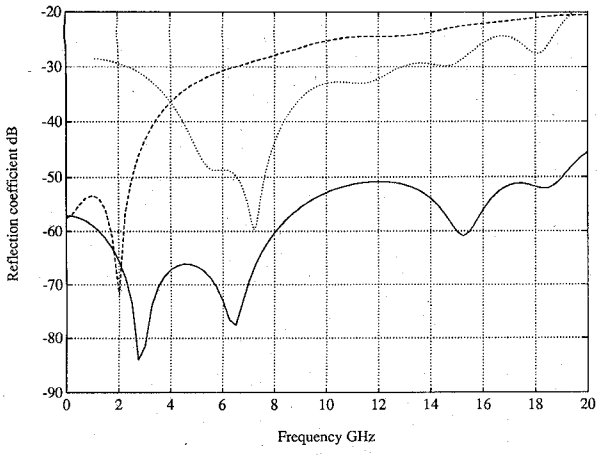

Fig. 3. Numerical experiment reflection coefficient for a microstrip line. Solid line: first order ABC, $\epsilon_{reff} = 7.12$. Dotted line: first order ABC, $\epsilon_{reff} = 8.12$. Dashed line: DBC, $\epsilon_{reff\,1} = 7.12$, $\epsilon_{reff\,2} = 8.50$.

tion domain for both DBC and Mur's boundary condition. In the DBC, $\epsilon_{reff\,1} = 7.12$ and $\epsilon_{reff\,2} = 8.50$ are used to determine the two velocities. In Mur's first-order ABC, $\epsilon_{reff} = 7.12$, 8.12 are used to determine the velocity, respectively. From this result we see that in the time domain the reflections from the computation domain boundary are greatly reduced using DBC: in fact, DBC reflections are an order of magnitude less than those from the first-order boundary conditions. The numerical reflection coefficients for both DBC and the first-order boundary conditions are given in Fig. 3. This figure shows that DBC absorbs the wave over a large frequency band, i.e., the reflection coefficient is less than −45 dB from 0 to 20 GHz, where $\epsilon_{reff\,1} = 7.12$ and $\epsilon_{reff\,2} = 8.50$ are used for the DBC. For the first-order condition, the reflection coefficients are less than −45 dB only over the ranges from 0 to 3 GHz when $\epsilon_{reff} = 7.12$, or from 5 to 8 GHz when $\epsilon_{reff} = 8.12$.

IV. Conclusion

The dispersive boundary condition allows the dispersion of waves to be incorporated into the design of an absorbing boundary condition. This feature can be very useful when the dispersion for a major outgoing wave is known. Both the validity and the efficiency of the DBC have been demonstrated by carrying out analyses on a microstrip line. With DBS, the memory requirement for FD-TD analyses of microstrip components and antennas can be greatly reduced.

The main difference between DBC and ABC is that DBC is designed to optimize the boundary condition according to the dispersion characteristics of waves, while ABC is designed to optimize the boundary condition according to the propagation direction of the waves. The introduction of the concepts which are the basis of DBC is specially important for study of absorption for strongly dispersive waves, such as occurs in conductor waveguides and dielectric waveguides. The further application of the proposed DBC to waveguide component analysis has been investigated in a separate paper [10]. Based on the ideas presented in this paper, some ABC's can be modified into DBC's.

References

[1] X. Zhang, J. Fang, K. K. Mei, and Y. Liu, "Calculations of the dispersive characteristics of microstrips by the time-domain finite-different method," *IEEE Trans. Microwave Theory Tech.*, vol. 36, pp. 263–267, Feb. 1988.

[2] X. Zhang and K. K. Mei, "Time domain finite difference approach to the calculation of the frequency dependent characteristics of microstrip discontinuities," *IEEE Trans. Microwave Theory Tech.*, vol. 36, pp. 1775–1787, Dec. 1988.

[3] G. Liang, Y. Liu, and K. K. Mei, "Full-wave analysis of coplanar waveguide and slotline using the time-domain finite-difference method," *IEEE Trans. Microwave Theory Tech.*, vol. 37, pp. 1949–1957, Dec. 1989.

[4] D. M. Sheen, S. M. Ali, M. D. Abouzahra, and J. A. Kong, "Application of the three-dimensional finite-difference time-domain method to the analysis of planar microstrip circuits," *IEEE Trans. Microwave Theory Tech.*, vol. 38, pp. 849–857, July 1990.

[5] J. Litva, Z. Bi, K. Wu, R. Fralich, and C. Wu, "Full-wave analysis of an assortment of printed antenna structures using the FD-TD method," *1991 IEEE AP-S Int. Symp. Dig.*, June 1991, pp. 410–413.

[6] C. Wu, K. Wu, Z. Bi, and J. Litva, "Accurate Characterization of planar printed antennas using finite difference time domain method," submitted to *IEEE Trans. Antennas Propagat.*

[7] R. G. Keys, "Absorbing boundary conditions for acoustic media," *Geophysics*, vol. 50, no. 6, pp. 892–902, July 1985.

[8] R. L. Higdon, "Numerical absorbing boundary conditions for the wave equation," *Math. Comput.*, vol. 49, no. 179, pp. 65–91, July 1987.

[9] R. L. Higdon, "Absorbing boundary conditions for difference approximations to the multi-dimensional wave equation," *Math. Comput.*, vol. 47, no. 176, pp. 437–459, Oct. 1986.

[10] Z. Bi, J. Litva, K. Wu, and C. Wu, "Dispersive absorbing boundary conditions (DBC) for waveguide component analysis using the FD-TD method," submitted to *IEEE Trans. Microwave Theory Tech.*

New Broadband Rectangular Waveguide with L-Shaped Septa

Pradip Kumar Saha and Debatosh Guha

***Abstract*—Rectangular waveguides with double L-shaped septa—variants of Double T-Septa Guides (DTSG) [1], [2]—have been analyzed theoretically and are proposed as new broadband waveguides. Results indicate that significant improvement in cutoff wavelength and bandwidth in particular should be available with L-shaped septa in antisymmetric configuration.**

I. Introduction

Recently rectangular waveguides with T-shaped septa have been proposed as alternative to ridged waveguides [1], [2]. Theoretical analysis using the Ritz–Galerkin technique showed that the lowest TE mode of such a guide has superior cutoff, bandwidth and impedance characteristics. It was further shown theoretically that dielectric loading of the septa-gap can improve the cutoff and bandwidth significantly [3]. Experimental verification of these properties and formulations of the problems by other methods have been reported in the literature [4]–[8].

In this paper we propose another type of broadband septum waveguides—a variant of the previously reported Double T-Septa Guide (DTSG) [1]. These guides have L-shaped septa located an-

Manuscript received November 7, 1991; revised September 10, 1991.

The authors are with the Institute of Radio Physics and Electronics, University College of Technology, 92, Acharya Prafulla Chandra Road, Calcutta 700 009, India.

IEEE Log Number 9106052.

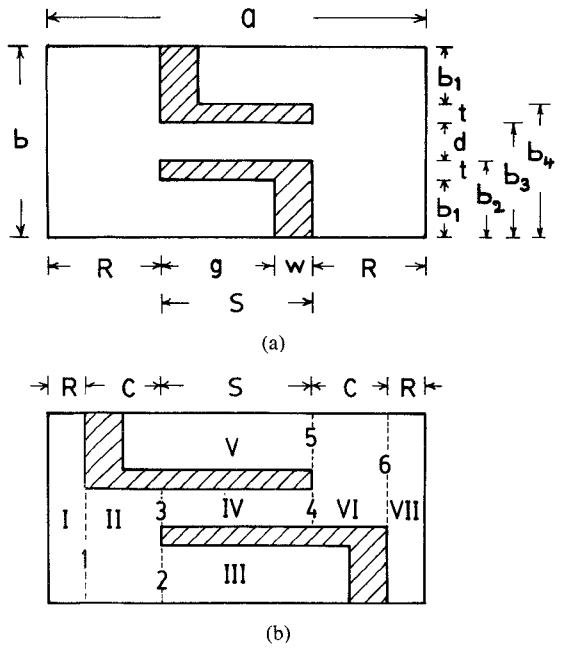

Fig. 1. (a) Double L-Septa Guide: DLSG1. (b) Double L-Septa Guide: DLSG2. The cross section is divided into subregions I–VII. The apertures are marked 1–6.

tisymmetrically as shown in Fig. 1. We propose to call them Double L-Septa Guides (DLSG). The guide in Fig. 1(a) has two completely overlapping septa and will be referred to as DLSG1. The other type, shown in Fig. 1(b), has two antisymmetric partially overlapping septa and will be referred to as DLSG2.

We present the theoretical cutoff and bandwidth characteristics of the dominant TE modes of the DLSG, compare with those of DTSG and examine the effect of partial overlapping of septa. The bandwidth is calculated from the cutoff wavelengths of the first two TE modes having their E-field polarized parallel to the Y-axis in the septa gap. We refer to them as the first and second bandwidth determining modes and refrain from using any modal nomenclature since the structures do not have any symmetry plane. These modes correspond to the TE_{10} and TE_{20} hybrid modes, respectively, of ridged [9] and T-septa waveguides [1]. The theoretical results indicate the possibility of marked improvement over the characteristics of DTSG when L-shaped septa are used in the proposed configurations.

II. Analysis

The TE eigenvalue equation of DLSG2 was derived using the Ritz–Galerkin technique as was done in the case of T-septa waveguides [1], [2]. The DLSG configurations consist of longitudinal aperatures cascaded in both X- and Y-directions and are treated by a variation of the analysis in [1]. The formulation basically involves the derivation of the coupled integral equations for the unknown electric fields over the apertures.

The steps involved in the analysis are outlined below.

1) In the seven different subregions of the cross section (Fig. 1(b)) the $h_z(x, y)$ and $e_y(x, y)$ components of the TE basis fields [9] are written in appropriate expanded forms.

2) Let the unknown aperture electric fields as functions of y be denoted by

(i) $E_1(y)$, $x = R$, $0 \le y \le b_3$

(ii) $E_2(y)$, $x = R + c$, $0 \le y \le b_1$

(iii) $E_3(y)$, $x = R + c$, $b_2 \le y \le b_3$

(iv) $E_4(y)$, $x = R + c + s$, $b_2 \le y \le b_3$

(v) $E_5(y)$, $x = R + c + s$, $b_4 \le y \le b$

(vi) $E_6(y)$, $x = a - R$, $b_2 \le y \le b$.

By matching $e_y(x, y)$ to the unknown electric field $E_i(y)$ over the ith aperture, $i = 1, 2, \cdots 6$, from left and right hand sides, the coefficients of expansions (in step 1) can be expressed in terms of E_i.

3) Six equations are obtained from the continuity of h_z over the apertures. When the expansion coefficients in these equations are eliminated by using the expressions derived in step 2, six coupled summation-integral equations are obtained.

4) To solve the integral equations by the Galerkin's method the following expansions of the unknown aperture fields $E_i(y)$ are substituted in the following equations:

$$E_{1(6)}(y) = \sum_{n=0}^{N_1} A_{1n(6)} \cos \frac{n\pi}{b_3} (y - b_{3(2)}) \tag{1}$$

$$E_{2(5)}(y) = \sum_{n=0}^{N_2} A_{2n(5)} \cos \frac{n\pi}{b_1} (y - b_{1(4)}) \tag{2}$$

$$E_{3(4)}(y) = \sum_{n=0}^{N_3} A_{3n(4)} \cos \frac{n\pi}{d} (y - b_2). \tag{3}$$

5) Then taking inner product of the equations with appropriate basis functions, the integral equations are transformed into six sets of homogeneous equations in the unknown coefficients A_{in}, $i = 1, 2, \cdots 6$ (see the Appendix).

Equations (A1)–(A6) can be put into matrix form

$$[F(k_c)]\underline{A} = 0 \tag{4}$$

where

$$\underline{A} = [\underline{A}_1^T \underline{A}_2^T \underline{A}_3^T \underline{A}_4^T \underline{A}_5^T \underline{A}_6^T]^T \tag{5}$$

and $[F]$ is a square matrix of size $2(N_1 + N_2 + N_3) + 6$. The TE eigenvalues are then given by the roots of the equation

$$\det [F(k_c)] = 0. \tag{6}$$

III. Results of Numerical Computation

Eigenvalues of the lowest and the first higher order bandwidth determining modes of DLSG2 were computed from the roots of (6). In (A1)–(A6) the parameters N_1, N_2 and N_3 determine the number of terms in the expansions of the electric fields in the apertures 1, 2 and 3, respectively and also 6, 5 and 4, respectively; M_1 and M_2 define the number of terms in the trough field expansions (subregions I and II, respectively, and also VII and VI, respectively). Computation of λ_{c1}/a and λ_{c2}/a, the normalized cutoff wavelengths of the first two bandwidth determining modes, was carried out with $N_1 = N_2 = N_3 = 10$ and $M_1 = M_2 = 20$. For these parameter values, the relative convergence effect was found to be insignificant for practical purposes.

Although DLSG1 can be looked upon as a special case of DLSG2 with $c = 0$, we refer to them as separate structures so that DLSG2 would denote configurations of partially overlapped septa ($c > 0$) only. For either structure the septa-width parameter s/a is defined as the normalized overlap width. In DLSG1, variation of s/a is accompanied by simultaneous variation of R/a such that $2R + s = a$ (constant), that is, the locations of the septa bases also change with the septa width. In DLSG2, however, R/a is kept fixed and

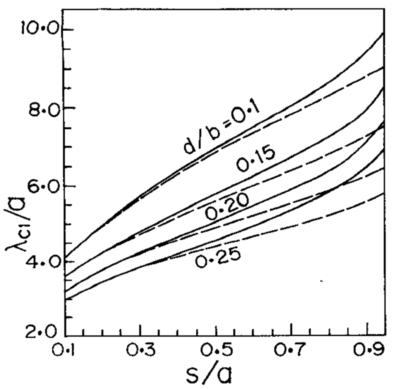

Fig. 2. Normalized cutoff wavelength λ_{c1}/a versus normalized septa width s/a. $b/a = 0.50$, $t/b = 0.05$, $w/a = 0.10$. ———— DLSG1, ----------- DTSG.

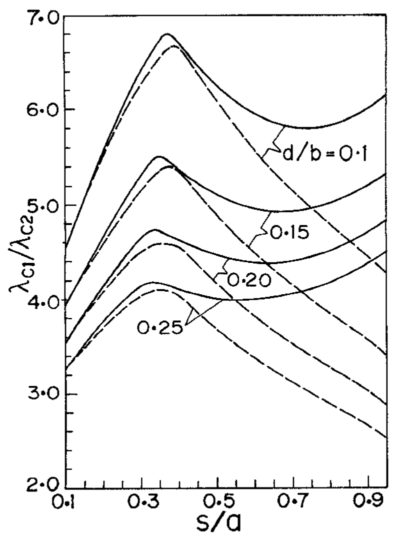

Fig. 3. Bandwidth $\lambda_{c1}/\lambda_{c2}$ versus s/a. $b/a = 0.50$, $t/b = 0.05$, $w/a = 0.10$. ———— DLSG1, ----------- DTSG.

the overlap width s/a is varied by changing the septa dimensions such that $s + 2c = a - 2R$ (constant).

Figs. 2 and 3 show the variation of λ_{c1}/a and bandwidth $\lambda_{c1}/\lambda_{c2}$, respectively, for DLSG1 together with those of DTSG [1] for comparison. The cutoff characteristics of the two structures are similar, DLSG1 showing larger values of λ_{c1}/a, particularly for large s/a and gap-width d/b. The bandwidth characteristics of the two structures are also not much different below $s/a = 0.4$. The DLSG1 peaks are slightly higher and a little shifted toward lower values of s/a compared to DTSG. But beyond the peaks and for higher values of s/a, the improvement in bandwidth with L-shaped septa is significant. The difference in the variation of the bandwidth of the two structures can be seen from the λ_{c2}/a versus s/a characteristics, shown in Fig. 4. The λ_{c2}/a of the two structures has nearly the same values up to $s/a = 0.4$ and then for DLSG1 it increases at a much slower rate than DTSG, thereby producing larger modal separation.

When compared with DLSG1, the λ_{c1}/a of DLSG2 (Fig. 5) shows further increase. The two curves coincide for the value of s/a which makes $c/a = 0$. This improvement is expected since for the same value of the septa-width parameter s/a, the DLSG2 configuration provides larger capacitive loading. The bandwidth

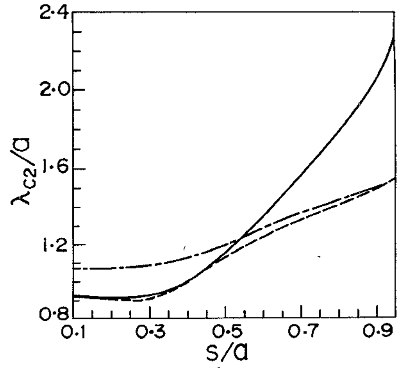

Fig. 4. Normalized cutoff wavelength versus s/a for the first higher order bandwidth determining mode. $b/a = 0.50$, $d/b = 0.20$, $t/b = 0.05$, $w/a = 0.10$. $R/a = 0.04$ for DLSG2. ———— DTSG, ----------- DLSG1, -·—·-·—·-·-·-·. DLSG2.

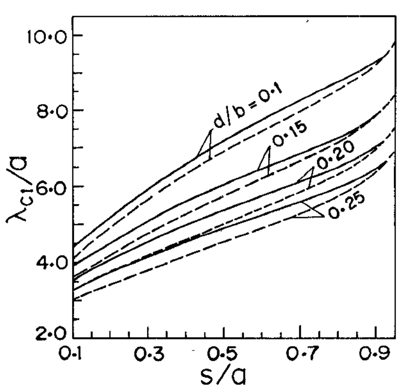

Fig. 5. λ_{c1}/a versus s/a of L-Septa guides. ———— DLSG2, ----------- DLSG1. Parameters as in previous figures.

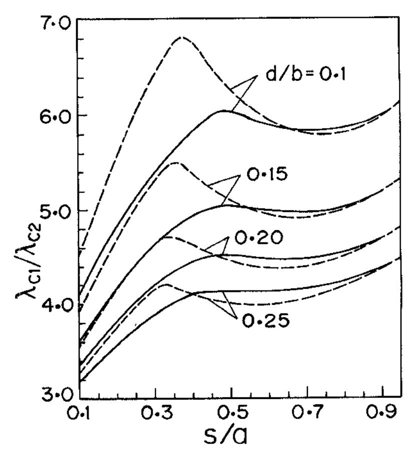

Fig. 6. $\lambda_{c1}/\lambda_{c2}$ versus s/a of L-Septa guides. ----------- DLSG1, ———— DLSG2. Parameters as in previous figures.

characteristics of DLSG2, however, depend on the additional parameter R/a. As shown in Fig. 6, for the particular chosen value of $R/a = 0.04$, the DLSG2 bandwidth is much lower for $s/a < 0.4$ and also shows less peaking. It becomes comparable to that of DLSG1 only for larger values of s/a, that is, when the DLSG2 configuration approaches DLSG1.

To find out if this deficiency of DLSG2 can be rectified, we examine the effect of the parameter R/a, that is, the location of the septa base while the septa overlap width s/a is held constant. As

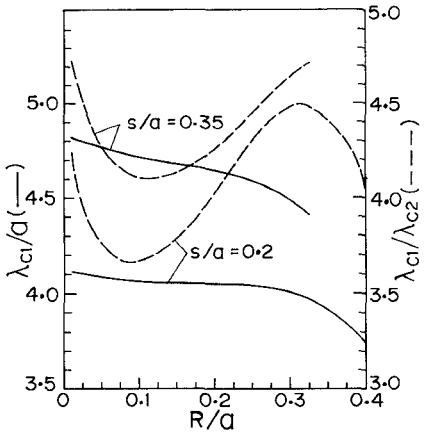

Fig. 7. Variation of λ_{c1}/a and $\lambda_{c1}/\lambda_{c2}$ with R/a for DLSG2. $d/b = 0.2$. Other parameters as in previous figures.

shown in Fig. 7, the λ_{c1}/a of DLSG2 increases slowly with decreasing R/a or increasing c/a, while the bandwidth shows a more pronounced variation. These results indicate that for small values of s/a, the DLSG2 bandwidth can be made to exceed that of DLSG1, although marginally, with suitable choice of R/a or c/a.

IV. Conclusion

New rectangular waveguides with two L-shaped septa attached to the broad walls in antipodal configuration have been examined theoretically. The cutoff and bandwidth characteristics have been derived by the Ritz–Galerkin technique and compared with those of Double T-Septa Guide reported earlier. With respect to both, the type DLSG1 offers significantly improved characteristics. Not only is the cutoff wavelength of the dominant mode larger, but the bandwidth, too, remains large over a wide range of values of the septa width s/a thereby simplifying the optimization problem. The cutoff and bandwidth characteristics of DLSG2 are not much different from those of DLSG1 for large values of s/a (>0.4). However, for smaller values of s/a, the characteristics of the two configurations can be made comparable by suitable choice of the parameter R/a or c/a.

Appendix

The six sets of homogeneous equations in the unknown coefficients A_{in}, $i = 1, 2, \cdots 6$, from which the eigenvalue (6) in Section II is derived, are given below:

$$\sum_{n=0}^{N_1} A_{1n}\left(\sum_{m=0}^{M_1} u_m I_{1pm} I_{1nm} + \delta_{np} t_p\right) + \sum_{n=0}^{N_2} A_{2n}(-r_p I_{2np}) + \sum_{n=0}^{N_3} A_{3n}(-r_p I_{3np}) = 0 \quad \text{(A1)}$$

where $p = 0, 1, 2, \cdots N_1$.

$$\sum_{n=0}^{N_1} A_{1n}(-r_n I_{2pn}) + \sum_{n=0}^{N_2} A_{2n}\left(\sum_{m=0}^{M_2} q_m I_{2pm} I_{2nm} + \delta_{pn} f_p\right) + \sum_{n=0}^{N_3} A_{3n}\left(\sum_{m=0}^{M_2} q_m I_{2pm} I_{3nm}\right) = 0 \quad \text{(A2)}$$

where $p = 0, 1, 2, \cdots N_2$.

$$\sum_{n=0}^{N_1} A_{1n}(-r_n I_{3pn}) + \sum_{n=0}^{N_2} A_{2n}\left(\sum_{m=0}^{M_2} q_m I_{3pm} I_{2nm}\right) + \sum_{n=0}^{N_3} A_{3n}\left(\sum_{m=0}^{M_2} q_m I_{3pm} I_{3nm} + \delta_{np} v_p\right) + \sum_{n=0}^{N_3} A_{4n}(-\delta_{np} w_p) = 0 \quad \text{(A3)}$$

where $p = 0, 1, 2, \cdots N_3$.

$$\sum_{n=0}^{N_1} A_{3n}(-\delta_{np} w_p) + \sum_{n=0}^{N_3} A_{4n}\left((-1)^{(p+n)} \sum_{m=0}^{M_2} q_m I_{3pm} I_{3nm} + \delta_{np} v_p\right) + \sum_{n=0}^{N_2} A_{5n}\left((-1)^p \sum_{m=0}^{M_2} q_m I_{3pm} I_{2nm}\right) + \sum_{n=0}^{N_1} A_{6n}(-(-1)^p r_n I_{3pn}) = 0 \quad \text{(A4)}$$

where $p = 0, 1, 2, \cdots N_3$.

$$\sum_{n=0}^{N_3} A_{4n}\left((-1)^n \sum_{m=0}^{M_2} q_m I_{2pm} I_{3nm}\right) + \sum_{n=0}^{N_2} A_{5n}\left(\sum_{m=0}^{M_2} q_m I_{2pm} I_{2nm} + \delta_{np} f_p\right) + \sum_{n=0}^{N_1} A_{6n}(-r_n I_{2pn}) = 0 \quad \text{(A5)}$$

where $p = 0, 1, 2, \cdots N_2$.

$$\sum_{n=0}^{N_3} A_{4n}(-(-1)^n r_p I_{3np}) + \sum_{n=0}^{N_2} A_{5n}(-r_p I_{2np}) + \sum_{n=0}^{N_1} A_{6n}\left(\sum_{m=0}^{M_1} u_m I_{1pm} I_{1nm} + \delta_{np} t_p\right) = 0 \quad \text{(A6)}$$

where $p = 0, 1, 2, \cdots N_1$.

Various terms in (A1)–(A6) are defined as follows:

$$k_{x1m}^2 + (m\pi/b)^2 = k_{x2m}^2 + (m\pi/b_3)^2 = k_{x3m}^2 + (m\pi/b_1)^2 = k_{x4m}^2 + (m\pi/d)^2 = k_c^2 = (2\pi/\lambda_c)^2$$

$$u_m = \cot k_{x1m} R/(\epsilon_m b k_{x1m})$$

$$r_m = (k_{x2m} \sin k_{x2m} c)^{-1}$$

$$q_m = r_m \cos k_{x2m} c/(\epsilon_m b_3)$$

$$t_m = q_m(\epsilon_m b_3)^2$$

$$w_m = \epsilon_m d/(k_{x4m} \sin k_{x4m} s)$$

$$v_m = w_m \cos k_{x4m} s$$

$$f_m = \epsilon_m b_1 \cot k_{x3m} g/k_{x3m}$$

$$\epsilon_m = 1 \ (m = 0); \quad 1/2 \ (m \neq 0)$$

$$I_{1ij} = \int_0^{b_3} \cos\frac{i\pi}{b_3}(y - b_3) \cos\frac{j\pi}{b}(y - b)\, dy$$

$$I_{2ij} = \int_0^{b_1} \cos\frac{i\pi}{b_1}(y - b_1) \cos\frac{j\pi}{b_3}(y - b_3)\, dy$$

$$I_{3ij} = \int_{b_2}^{b_3} \cos\frac{i\pi}{d}(y - b_2) \cos\frac{j\pi}{b_3}(y - b_3)\, dy.$$

References

[1] G. G. Mazumder and P. K. Saha, "A novel rectangular waveguide with double T-septums," *IEEE Trans. Microwave Theory Tech.*, vol. MTT-33, pp. 1235–1238, Nov. 1985.

[2] ——, "Rectangular waveguide with T-shaped septa," *IEEE Trans. Microwave Theory Tech.*, vol. MTT-35, pp. 201–204, Feb. 1987.

[3] ——, "Bandwidth characteristics of inhomogeneous T-septum waveguides," *IEEE Trans. Microwave Theory Tech.*, vol. MTT-37, pp. 1021–1026, June 1989.

[4] Y. Zhang and W. T. Joines, "Some properties of T-septum waveguides," *IEEE Trans. Microwave Theory Tech.*, vol. MTT-35, pp. 769–775, Aug. 1987.

[5] ——, "Attenuation and power-handling capability of T-septum waveguides," *IEEE Trans. Microwave Theory Tech.*, vol. MTT-35, pp. 858–861, Sept. 1987.

[6] R. R. Mansour and R. H. Macphie, "Properties of dielectric loaded T-septum waveguides," *IEEE Trans. Microwave Theory Tech.*, vol. 37, pp. 1654–1657, Oct. 1989.

[7] F. J. German and L. S. Riggs, "Bandwidth properties of rectangular T-septum waveguides," *IEEE Trans. Microwave Theory Tech.*, vol. 37, pp. 917–919, May 1989.

[8] B. E. Pauplis and D. C. Power, "On the bandwidth of T-septum waveguides," *IEEE Trans. Microwave Theory Tech.*, vol. 37, pp. 919–922, May 1989.

[9] J. P. Montgomery, "On the complete eigenvalue solution of ridged waveguide," *IEEE Trans. Microwave Theory Tech.*, vol. MTT-19, pp. 547–555, June 1971.

Matrix Theory Approach to Complex Waves

Michal Mrozowski and Jerzy Mazur

Abstract—**Complex waves in shielded lossless inhomogeneous isotropic guides are investigated. A critical appraisal of the existing theory of complex waves is given and new approach is proposed. A mathematical condition for the existence of complex waves is derived using the properties of a generalized symmetric matrix eigenvalue problem. It is shown that complex waves may exist in slightly perturbed homogeneous guides as a result of the coupling of a pair of degenerate or nearly degenerate modes.**

I. Introduction

Complex waves are the modes guided by shielded lossless guides which have complex propagation constants despite the lossless nature of the structure. A first theory of complex waves was published by Chorney as early as in 1961 [7], in a research report devoted to the properties of waves supported by anisotropic bidirectional guides. Complex waves do not exist in hollow cylindrical guides and initially it was believed that lossless shielded uniform dielectric guides can not generally support modes with complex propagation constants [6]. Pioneering work by Clarricoats and coworkers [14]–[16] proved that complex waves can be excited in a circular waveguide containing a coaxial dielectric rod. Similar result was obtained independently by Belyantsev and Gaponov [9] who discovered complex waves in coupled lines. Since then complex and backward waves in a circular waveguide containing a dielectric rod have been the subject of thorough numerical investigations [14]–[23]. It was established that complex waves may only be excited if the permittivity of the dielectric rod is high enough. It was also found that a complex wave carries no power and the existence of complex waves was finally confirmed experimentally [4]. These detailed studies published now and again in the literature were accompanied by theoretical consideration which gave deeper insight into the nature of complex waves [5], [8].

In the 1980's the scope of the research into inhomogeneous guides broadened and complex waves were reported for a variety of waveguiding structures including dielectric image guide [24]–[25], microstrip [27], [31], [32] and fin line [10], [31]. An interesting result was obtained by Omar and Schünemann [12], [13] who proved that although a single complex wave carries no power, two complex waves forming a pair are not orthogonal with respect to cross power and consequently a pair as a whole behaves as a mode below cutoff carrying purely reactive power. It was also found that in certain structures, for instance in a rectangular image guide investigated by Strube and Arndt [24], it is possible to obtain complex waves even if the perturbation caused by inhomogeneity is relatively small. The attention which complex waves have received recently is primarily due to the role which they play in the discontinuity analysis. Investigations have shown that complex waves constitute an essential part of modal spectrum and their omission may lead to erroneous results in certain discontinuity problems [12], [28]–[31].

The intensive studies into the complex waves resulted in 1987 in a paper [13] by Omar and Schünemann which was intended as a general treatment of complex waves. Omar and Schünemann's 1987 paper use the approach similar to the one used in Chorney's 1961 report. In both cases the original boundary value problem was converted into a matrix eigenvalue problem but using slightly different techniques (It can be shown [33] that the two approaches are identical for infinite matrix dimensions). Chorney concentrated his work on the derivation of integral relations for complex waves. Omar and Schünemann proposed using the symmetry of the characteristic matrix as a criterion for the existence of complex waves. In this contribution we will show that some of Omar and Schünemann's conclusions are premature and propose a more rigorous approach to complex waves.

II. Mathematical Formulation

As a departure point for the analysis we shall use the matrix formulation derived by Omar and Schünemann [13] who investigated a general lossless structure of a uniform waveguide inhomogeneously filled with a dielectric whose relative permittivity was a function of transverse coordinates ($\epsilon_r = \epsilon_r(r)$). The fields in the guide were assumed to have the z dependence in the form $e^{-j\beta z}$, and expanded in series of normalized longitudinal components of TM and TE modes existing in the empty waveguide [11], [13]. The expansion coefficients and the propagation constants of the modes supported by the loaded guide can be obtained from the following matrix eigenvalue equation (eq. 12 in [13]):

$$\begin{bmatrix} (k_0^2\underline{\underline{I}} - \underline{\underline{S}}^{-1})\underline{\underline{R}}^e & -\omega\mu_0/\lambda(k_0^2\underline{\underline{I}} - \underline{\underline{S}}^{-1})\underline{\underline{T}} \\ -\omega\epsilon_0\lambda\underline{\underline{T}}^T & k_0^2\underline{\underline{R}}^h - \underline{\underline{\Lambda}}^h \end{bmatrix} \begin{bmatrix} \underline{A}' \\ \underline{B}' \end{bmatrix} = \beta^2 \begin{bmatrix} \underline{A}' \\ \underline{B}' \end{bmatrix} \tag{1}$$

Manuscript received February 21, 1990; revised August 18, 1991. This work was supported by the British Council under the British Council Fellowship Scheme and the Polish Academy of Sciences under contract CPBP-02.02.3.2.

The authors are with the Technical University of Gdansk, Telecommunications Institute, Majakowski Str. 11/12, 80-952 Gdansk, Poland.

IEEE Log Number 9106051.